Management of Manufacturing, Quality, Curing, Repair and Life Prognosis of Aircraft Composite Structures

C. Keulen, F. Melemez, T. Boz, H. Turkmen, M. Cassi, M. Yildiz, A. Suleman
University of Victoria
Victoria, B.C., V8W 3P6
CANADA

suleman@uvic.ca

ABSTRACT

Composite materials are becoming increasingly more valuable in the transportation industry as they offer lighter weight options to traditional metallic structures. More than 20% of the Airbus A380 is made of composites and over 50% of the upcoming Boeing 787 are currently being made of composite. Most composite materials are composed of a number of plys of reinforcement fiber that are laminated together. The orientation of these fibers has a great impact on the material properties of the structure, specifically the stiffness and strength. This also has a major influence on the speed that vibrations travel through the material, which is relevant to various types of SHM such as ultrasonic or Lamb wave based techniques. The nature of composites being composed of multiple materials and the laminated structure allows for various damage and failure modes. Generally composites are more susceptible to damage caused by impact. Separation of plys, also known as delamination can occur below the surface with no visible evidence. These delaminations can grow over time eventually resulting in catastrophic failure with little warning.

Optical fibers have the ability to be seamlessly embedded inside composite materials. Due to their small diameter and similar material properties fiber optics have very little effect on the host material properties. Once embedded in the composite, the optical fiber is protected from the environment and exposed to the same temperatures, strains and fields (magnetic, electric) that the material is exposed to. This opens a wide range of opportunity for the combination of optical fiber sensors and composite materials.

1.0 APPLICATION OF EMBEDDED FIBER OPTICS

Composites, compared to metallic materials, present relatively difficult processing characteristics and damage assessment. Fiber optics can be used during the processing and service stages of component life to mitigate these drawbacks. In the case of liquid composite molding, such as resin transfer molding or vacuum infusion, fiber optic sensors can be used to determine the presence of resin and indicate the location of dry spots where the resin has not saturated. The same sensors can be used during the resin curing stage to monitor the degree of cure and accurately indicate when the resin is fully cured and ready to be removed from the mold. When in service, the sensors can be used to monitor the strain in a structure and incorporated into an integrated structural health monitoring system.

The Lecture Series notes focus on the application of fiber optic sensors embedded into composite structures and how they can be implemented and utilized for the processing and manufacturing of aircraft structural components, subsequently for the operational and service stage of the composite component and finally to predict the remaining useful life. Finally, a study is presented to characterize the behavior of the CFBG sensor and analyse its applicability to the structural health monitoring of repaired composites. More specifically, the capability of detecting the presence of a patch debond and evaluating its size is examined.

1.1 Flow Monitoring During Resin Infusion

Embedded fiber optic sensors have some important applications to the field of liquid composite molding (LCM). Liquid composite molding includes composite material processing techniques such as resin transfer molding (RTM) and vacuum assisted resin transfer molding (VARTM) also known as vacuum infusion molding. With these processes, a pressure differential is used to saturate dry fiber reinforcement with resin in either a two sided mold as with RTM or a one sided mold as with VARTM. This phase is known as the infusion phase. Complete saturation of the fiber reinforcement is critical for a part to be acceptable. Generally speaking the resin is allowed to saturate the part until the operator deems it complete and shuts off the resin supply. Since most molds are opaque, it is impossible rarely known with certainty whether or not the part is saturated. With small thin parts it can be assumed with reasonable certainty that the part is fully saturated or when the process has been run a number of times with success. However, when a process is being designed or tested for the first time, there is a lot of uncertainty.

Some fiber optic sensors have the ability to sense the presence of resin. These sensors can be embedded inside the fiber reinforcement to sense when the resin has completely saturated the part. With this knowledge the infusion can continue until the sensors indicate that the part is complete before the infusion is stopped, ensuring that the part is fully saturated. This reduces wasted material from infusing the resin for too long or parts that are not fully saturated that must be discarded or reworked. This also gives the manufacturer a higher degree of certainty that the parts are free of hidden voids that would affect the integrity of the part and reduce quality control requirements later on down the line. Taking this technique one step further, part of the processing could be automated by connecting the sensors to a control system that uses them to control the mold; opening and closing inlets and outlets in order to optimally infuse the part then allowing the resin to cure and automatically unload the part. Mainly due to the wide spread use of prepreg materials in aerospace, resin flow front detection has been investigated less than cure and health/damage monitoring, however many researchers have used fiber optics to detect the flow front of resin during LCM processes.

1.2 Cure Monitoring

Once a part is fully infused the resin must cure before it may be removed from the mold. In most liquid composite molding techniques, the cure phase takes the longest and is considered the bottleneck when trying to increase process efficiency. The chemical reaction that takes place when the resin is curing is exothermic which means it produces heat. As the resin cures the temperature inside the part raises steadily until it reaches a peak then starts to cool down. With most resins, after the temperature has reached a maximum the part is ready to be removed from the mold thereby allowing the mold to be used for the next part. If the temperature inside the part is monitored the peak may be detected and the part can be removed at an optimal time rather than basing the removal on a predetermined amount of time which can vary depending on the atmospheric conditions such as temperature and humidity. Fiber optic sensors that sense temperature can be embedded in the part and used for this very purpose. Other parameters can be used to monitor such as refractive index or viscosity.

A number of direct methods for characterizing the degree of cure currently exist. Traditional methods are based on thermal and dynamic analysis. Other techniques including the addition of photochromic, thermochromic compounds, or other dyes to the resin. Changes of color, absorbance and transmittance dependent upon time and temperature during cure can be monitored and correlation of spectral changes in the resin with polymerization and cross-link density can be made. Electrical resistance measurements and dielectric analysis techniques have also been successfully used to determine the completion of cure by monitoring capacitance, dissipation and DC electrical resistance of the resin.

The drawback of the aforementioned techniques is that they cannot make local measurements, only global. This is a concern as the degree of cure can vary throughout the composite due to factors such as thickness, fiber packing or thermal gradients induced by uneven mold heating. Some of these techniques also require

the resin to be in a neat form (only resin, no reinforcement fiber) or the addition of chemicals that remain in the resin after cure, which can negatively impact the composite. To overcome these issues, dielectric probes have been designed that measure the degree of cure in a local area. The disadvantage of these probes, however is that they are intrusive when embedded within the composite thereby rendering the composite unfit for service.

1.3 Structural Health Monitoring

Composites can also benefit from embedded optical fiber sensors while in service in the form of structural health monitoring (SHM). They can allow for higher performance parts that are safer and cheaper to produce and maintain. Embedded fiber optic strain sensors can give real time strain readings that can be used for a variety of purposes such as the physical condition of a structure, control or maintenance. Critical aircraft parts can be monitored and replaced when needed rather than after a predetermined number of cycles when they have reached their theoretical life. Since the strain in these parts is known in real time, they may be designed with lower safety factors therefore reducing weight and increasing performance. This also reduces the cost to produce the parts since less material is required. They are also safer for the end users because they are constantly monitored. Parameters that are monitored include the detection of impact damage and delamination, structural strains, crack propagation in bonded repair systems, temperature and fatigue induced damage.

There has been an enormous amount of research done on fiber optic based structural health monitoring of composite materials. Many techniques, sensors and interrogation schemes have been investigated. With the increased popularity of FBGs in the last decade, most of the more recent research is based on systems that use these sensors with effort put into development of high speed interrogation techniques, signal interpretation algorithms and integration.

In its most basic form, fiber optic based SHM of composites involves simply monitoring the strain in the material. Early research was done on interpreting strain measurements to determine the shape of a structure. Research was also done on comparing the response of undamaged to damaged specimens in an attempt to extract information pertaining to the size, type and location of the damage. Monitoring the progression of cracks and delaminations in unrepaired and repaired/patched composite structures and patches is also an area of interest.

Research into the detection of impact damage began in the late nineties. Much research has been conducted on ultrasonic based SHM as it shows a lot of potential as a method of determining the location and characteristics of damage. The basic technique involves Lamb waves that are generated at a given point in the structure and sensed at another. Characteristics such as propagation speed, wave mode, frequency, direction and magnitude are sensed and used to determine pertinent information about the structure. The waves are generally initiated by a piezoelectric actuator with frequencies in the range of kHz to MHz.

2.0 REMAINING USEFUL LIFE OF COMPOSITE STRUCTURES

A new technique for prediction of the Remaining Useful Life (RUL) of composites under fatigue loading using embedded FBG sensors will be discussed during the Lecture Series. The goal is to determine the RUL of a composite material using data obtained from embedded FBG sensors during the life of a structure. An estimate is made on the remaining life at every cycle based on data collected from the sensors and the previous loading history. This involves selecting an appropriate fatigue life prediction model that is compatible with the data obtained from FBGs and implementing this model to accurately predict the remaining useful life.

2.1 Theory

Research into the detection of damage using embedded fiber optic sensors has been performed by various researchers [3]. Doyle et al were among the first to monitor the reduction in stiffness of composites during fatigue with an FBG [4].

Many researchers have attempted to characterize the change in the reflected spectrum of an FBG to detect and measure the density of cracks based on the fact that a non-uniform strain distribution along an FBG causes broadening of the reflected spectrum [5-7]. Takeda et al attempted to correlate crack density with spectrum broadening using a theoretical model for crack density [5]. Yashiro et al, proposed a numerical approach to correlate the reflected spectrum of the embedded FBG sensor to damage [6]. Takeda et al subsequently proposed a method of addressing multiple damages near a stress concentration by a technique based on a layer-wise finite element analysis with cohesive elements [7]. Other techniques based on ultrasonic Lamb waves have also shown promise [8]. These generally involve the use of piezoelectric transducers that send surface waves through the material while FBG sensors are used to detect the waves.

An FBG is a segment of a single mode optical fiber core with a periodically varying refractive index in the axial (longitudinal) direction [9]. It allows a broad band of light to pass while reflecting a narrow band centered around a wavelength known as the Bragg wavelength, $\boldsymbol{\lambda_B}$. The periodic modulation of the refractive index at the grating location will scatter the light traveling inside the fiber core. Out of phase, scattered waves will form destructive interference thereby canceling each other while in phase light waves will add up constructively forming a reflected spectrum. The reflected wavelength depends on the grating pitch (spacing between the refractive index variations), Λ and the variation in refractive index, n. An FBG satisfies the Bragg condition as $\lambda_B = 2n\Lambda$. The change in spacing of the periodic refractive index modulation is a function of both strain and temperature. If an FBG sensor is under a mechanical load or temperature variation, the spacing and average refractive index will change, therefore causing a shift in the Bragg wavelength $\lambda_B(n,\Lambda)$. The sensitivity of strain and temperature of a bare FBG is 1.2pm/με and ~13.7pm/°C [9] however it is prudent to measure the strain and temperature sensitivity of every embedded FBG as factors such as variation in material properties and manufacturing tolerance will affect the sensitivity.

Fatigue of composites has been an area of interest for over forty years. The fatigue behavior of composites is a complex phenomenon due to various types of damage that can occur (fiber fracture, matrix cracking, fiber buckling, fiber-matrix interface failure, delamination, etc.) and interact with each other [10]. Research has shown that the damage process in fiber reinforced composites under fatigue loading is progressive and is a combination of various damage modes. The field of fatigue life modeling of composite materials is extensive, however there is still no widely accepted model that most engineers agree upon. Many excellent references that cover a variety of available models exist such as [10-12] among others.

As observed by various researchers, the effect of fatigue on the stiffness of fiber reinforced polymer matrix composites follows a trend. This trend can be characterized by three stages as shown in Figure 1. Stage I is characterized by a sharp, non-linear decrease in stiffness. This is attributed to a rapid interconnection of matrix cracking initiated by shrinkage stresses, degree of resin cure, voids and fiber discontinuities. This stage is generally limited to the first 15-25% of fatigue life. Stage II is characterized by a gradual, linear decrease in stiffness that occurs between 15-20% to 90% of the fatigue life. This decrease is attributed to matrix cracking leading to crack propagation, fiber debonding and delamination. The final stage shows a sharp non-linear decrease eventually resulting in a sudden fiber failure [13]. Interestingly, the very initial stages of fatigue testing results in an increase in stiffness that is generally attributed to viscoelastic deformation of the matrix allowing for fiber alignment along the axis of loading [14].

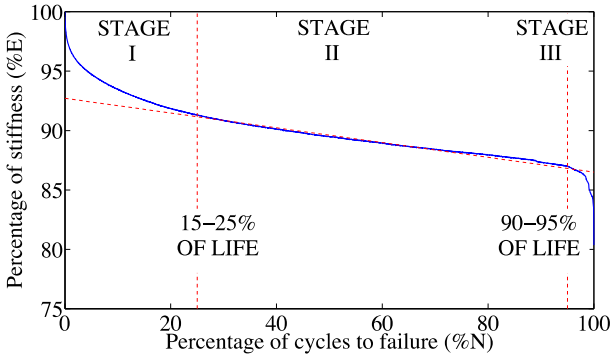

Figure 1: Stiffness degradation vs. fatigue cycle.

Researchers have shown that S-N curves of unidirectional composites have virtually no clear threshold stress level as established in metals however, it is recognized that a certain threshold level of strain in resin does exist for indefinite fatigue life although it is very low, around 5-10% of the ultimate strain [13]. Hence, life prediction models based on S-N curves may not be applicable for fiber reinforced plastic (FRP) composite materials.

Most models take factors such as stress, strain, stiffness and number of cycles and develop abstract material properties to develop a formulation. Other researchers have investigated other properties as an indication of fatigue. The challenge with these models is that they all require knowledge of the load/stress applied to the composite. With FBG sensors, this data is not available, only the strain is sensed.

The relevant data collected from an FBG is in the form of strain and number of cycles. As described above, the stiffness of composite materials under fatigue loading gradually decreases over time. This means that the modulus of elasticity is not constant, it is a function of the load history and the stress-strain relationship (Hooke's law) can no longer be applied to extract the magnitude of stress from strain. Therefore a suitable model cannot use stress as an input; it must use the strain.

A promising method of predicting the remaining useful life using only strain was developed by Natarajan et al [13]. The method relies on the strain energy release rate and takes advantage of the fact that it is linear throughout Stage II. It follows a similar approach to the fatigue modulus concept proposed by Hwang and Han [19].

To apply this model the material must be characterized to obtain a relationship between applied strain, ultimate strain and the energy release rate. The method assumes that there is a specific amount of strain energy in the material that is released before it enters Stage III, at which point it is past its useful life. The strain energy can be determined before fatigue loading and used to predict the number of cycles to failure. An example of the progression of the release of strain energy from a composite during fatigue is shown in Figure 2. This method can be employed as a cumulative model if the energy is summed over each cycle. Here, it is proposed to use this method to calculate the released energy on a per-cycle basis using strain data obtained from embedded FBGs to predict the remaining life. The complete derivation of this method is presented in [13]. An abbreviated version is presented here along with a modification so it can be applied to FBG acquired strain/cycle data.

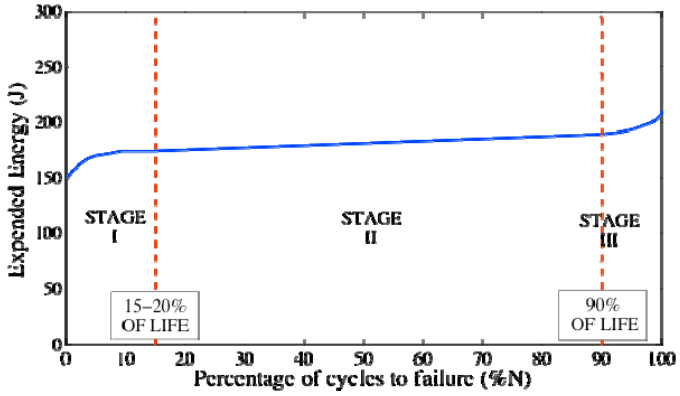

Figure 2: Expended strain energy during fatigue loading.

The data obtained during fatigue loading should be load and deflection. This data is then used to calculate the strain energy U_n at any cycle. The amount of energy released at 90% of the life cycle (when the material enters Stage III) compared to the initial amount of energy changes based on the ratio: $r = U_f/U_0$. Failure is assumed to occur at this point as the material is no longer intact and dangerously close to catastrophic failure, therefore: $N_f = N_{90\%} = 0.9N_{ult}$.

The slope of Stage II is the expended energy per cycle or the energy release rate: dU/dN. This can be obtained for each specimen by performing a regression analysis of the expended energy data in Stage II. The energy release rate is found to be constant and is characteristic of the constitutive material under similar loading conditions and increases with an increase in induced strain.

Experimental data of the variation in energy release rates with normalized maximum induced strain is fit to a power law:

$$\frac{dU}{dN} = a\left(\frac{\varepsilon_{max}}{\varepsilon_{ult}}\right)^b \qquad (6)$$

where ε_{max} is the maximum induced strain of the material, ε_{ult} is the ultimate static strain of the material (assumed to remain constant throughout the lifetime) and *a* and *b* are fatigue coefficients.

Since the coefficients a and b are invariant for a particular material under a given load type, the fatigue life can be written as:

$$N_f = \frac{U_0 - U_f}{a(\varepsilon_{max}/\varepsilon_{ult})^b} \qquad (7)$$

where U_0 is the initial strain energy of the material at ε_{max} before fatigue loading, U_f is the sum of the expended strain energy at the end of Stage II and N_f is the fatigue life just before entering Stage III.

Since the specimen is loaded linearly up to the mean strain level before applying fatigue load, the expended energy of the material before fatigue loading is the energy at the mean level. The energy of the material at 0 cycles can be written as:

$$U_0 = \frac{P_{mean}^2 l}{2AE} \qquad (8)$$

where P_{mean} is the mean level of the cyclic load, E is the modulus of elasticity in the loading direction, l is the span (gage length) and A is the cross sectional area. The fatigue life of a material can be obtained experimentally for a particular loading from Equations (2) and (6), at N_f and written as:

$$N_f = \frac{U_0 - rU_0}{a(\varepsilon_{max}/\varepsilon_{ult})^b} = \frac{(1-r)U_0}{a(\varepsilon_{max}/\varepsilon_{ult})^b} \quad (9)$$

Life prediction can be accomplished by summing the energy released under various load amplitudes for the corresponding number of cycles and finding $\mathbf{N}_f$ after inserting the total expended energy into Equation (9). In the case of an FBG based SHM system, the magnitude of the strain is sensed on every cycle. With this method it is possible to sum the energy on a cycle-by-cycle basis using data obtained from the FBG.

To calculate the energy released during one cycle, Equation (6) is integrated with respect to N over one cycle, i.e. from N_j to N_{j+1} and ε_{max} is replaced with $\varepsilon_j^{(FBG)}$, the maximum strain value recorded by the FBG during cycle j. This leads to:

$$\Delta U_j = a\left(\frac{\varepsilon_j^{(FBG)}}{\varepsilon_{ult}}\right)^b \quad (10)$$

The energy released during each cycle can then be summed during the life of the composite to get the total expended energy up to that cycle. The remaining life can be estimated: $\mathbf{U}_{remaining} = (1-\mathbf{r})\mathbf{U}_0 - \mathbf{U}_{expended}$, where $\mathbf{U}_{remaining}$ is the remaining energy left in the material before failure. Equation (7) can be modified to convert the remaining energy into the number of remaining cycles:

$$N_{n-f} = \frac{U_{remaining}}{a(\varepsilon_{expected}/\varepsilon_{ult})^b} \quad (11)$$

where N_{n-f} is the remaining life at cycle n, $\varepsilon_{expected}$ is the expected strain level for the remainder of the life. For example, $\varepsilon_{expected}$ could be the average maximum strain from the previous portion of life or if the component was expected to be under harsher loading, "$_{expected}$ would be greater than the average maximum strain. With Equation (11) various fatigue cycle scenarios could be predicted for various loading cycles by modifying the value of $\varepsilon_{expected}$. The addition of Equations (10) and (11) to the fatigue life prediction technique developed by Natarjan [13] allow for a stepwise addition of expended energy. This is a novel approach to remaining useful life prediction that allows a prediction to be made at each cycle.

2.2 Experimental Verification

Experimental validation was performed to explore the potential of this technique. This involves producing fatigue specimens with and without embedded FBG sensors, testing them to characterize the material then testing and applying the failure model to specimens that contain embedded FBGs.

A number of processing methods exist for composite materials. One method that is particularly suitable to produce composite parts satisfying stringent specifications of the aircraft industry is the Resin Transfer Molding (RTM) technique. RTM can produce high quality near net-shape parts with high fiber volume fractions, two high quality surfaces and little post processing in a fully contained system that eliminates human operator exposure to chemicals and reduces the chance of human error. For these reasons RTM has been selected to produce the specimens for this study. A laboratory-scale apparatus has been designed and built with the ability of embedding fiber optics into the composite component. This apparatus is used to produce at panels 620mm x 320mm x 3:5mm that are processed into specimens for fatigue testing.

A special fixture is required to grip the specimen such that the fiber optic ingress location is not under load. The fixture consists of three steel plates, a bar and a pin. Two plates are clamped across either side of the specimen with bolts. One plate has a slot that allows the fiber to egress from the composite. The plates are screwed into the third plate that has a cylindrical pin that interfaces with the machine grips. A stiffening bar is located across the slot to reduce detection when the bolts are tightened.

2.3 Results and Discussion

A total of 11 static tests and 33 fatigue tests were performed. Static tests were performed in order to determine the ultimate stress and strain of the material that was later tested under fatigue. The ultimate stress and strain were found to be 318.75MPa and 16.31mε, respectively where m_ε is milli-strain.

Once the static tests were complete, the fatigue tests were performed. Peak strain and load data was converted into expended energy per cycle and plotted to produce an energy curve for each specimen. The aforementioned energy release trend is quite apparent in the energy curve plots; an example plot is shown in Figure 2.

Linear regression was used to obtain the energy release rate (dU=dN) throughout the linear region. The energy release rate was plotted vs. normalized induced strain. This data was averaged, plotted and fit to a power law curve to obtain the values for fatigue coefficients a and b, of 14.67 and 0.070595, respectively. With a and b determined, the fatigue life could be predicted using Equation (9). The experimental and predicted results were plotted as an ε-N curve.

Figure 3 shows a plot of the surface temperature of Specimen 3-1 on the left vertical axis and the applied load on the right vertical axis vs. percent of test. They are presented on the same plot in order to compare their similar trends. The temperature data (blue) shows a sharp increase during the first ~5%. This is due to the autogeneous heating that occurs. After the initial peak there is a nonlinear decrease until ~18% . After that there is some erratic fluctuation from _18% to 55% which is likely due to external effects such as ambient temperature change. After that the decrease remains steady and linear until 95% when there is a final change to a greater decrease in temperature until failure. The load follows a very similar pattern aside from the initial sharp increase. From the first cycle to ~15% there is a nonlinear decrease before a constant linear decrease is observed until ~95% when a sharp nonlinear decrease occurs until failure.

Both data sets follow the trend of strain energy outlined in [13]. The temperature change is caused by the work done on the material. When there is a greater load applied then more strain energy is put into the material and therefore more autogeneous heating occurs. As the material starts to degrade and requires less load to reach the specified strain, less energy is put into the material and less heating occurs. Naturally there is a lag in the temperature signal due to the poor conductivity of glass fiber/epoxy composite. This suggests that while susceptible to external environmental effects, monitoring the surface temperature of composites subjected to fatigue may be used to give insight into the condition of the material.

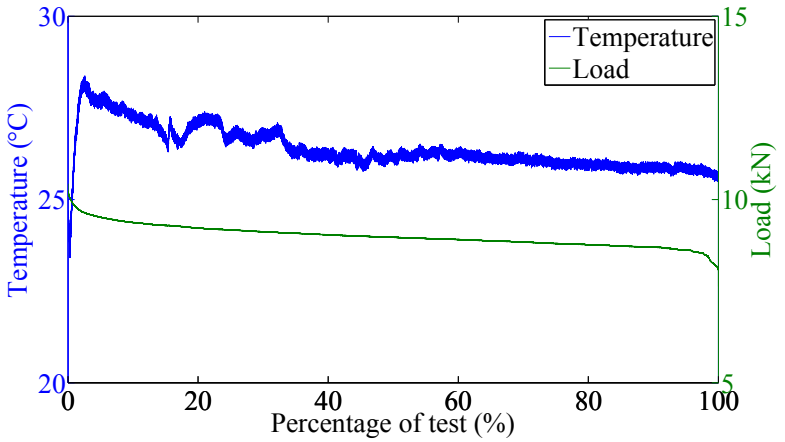

Figure 3: Temperature and load vs. percent of test.

After testing a total of 11 specimens statically and 33 in fatigue, the fatigue coefficients required to apply the strain energy release rate prediction model to a $[0/90]_{6s}$ glass fiber/epoxy laminate were obtained. In order to explore the concept of using FBGs to predict the remaining cycles throughout the fatigue life, three specimens with embedded FBGs were tested. The results of the non-FBG embedded fatigue tests closely agreed with previous work by Natarjan [13] showing the same material degradation pattern.

The introduction of Equations (10) and (11) to the fatigue life prediction technique developed by Natarjan [13] are novel, as is their approach to remaining useful life estimation that allows a prediction to be made at each cycle.

The conclusions drawn from these tests suggest that a more accurate and reliable signal from the embedded FBGs is required for accurate results. Three avenues to pursue in order to achieve this are: operate at lower strain level, investigate the use of shorter FBGs (1 - 3mm in length) and develop a more robust FBG interrogation algorithm. The ε_{ult} of carbon fiber is much lower than that of glass fiber meaning a structure composed of carbon fiber would see less strain and therefore an embedded FBG would not degrade as rapidly. To investigate this, the same study should be repeated with carbon fiber rather than glass fiber composites.

3.0 SHM OF COMPOSITE PATCH REPAIRS USING OPTICAL SENSORS

Over the years, researchers have concentrated their efforts on providing reliable SHM techniques that involved parts that, for their nature, are more difficult to inspect or more prone to suffer damage growth. As one can easily imagine, repairs are fully inside these categories.

In critical components or parts where non-destructive tests are difficult to perform or whose behavior is not yet entirely known, such as joints or adhesively attached patches, it is of extreme importance to find health monitoring systems that may reduce to acceptable levels the penalizing safety factors. A structural health monitoring strategy for patch repairs of carbon/epoxy structures was studied and implemented.

The functioning of Chirped Fibre Bragg Grating sensors was analyzed with gradual heat tests, evaluating their capability of sensing the presence of strain field variations through their physical length. The final objective was being able to obtain from the only information given by the reflection spectrum from the sensor the presence of a patch debond, and estimating its size with acceptable accuracy. From the calibration charts and tables prepared two methods to achieve this goal were extracted. The same sensors were placed

and embedded into patches, and the two methods were tested experimentally. As a support for the tests, an FEA analysis of the problem was carried out, supported in turn by tensile tests for material characterization. Good results were obtained from the experiments, confirming in the realistic setup approximately the same intrinsic errors that were encountered when the methods were designed.

3.1 Repair of Composite Structures

With the diffusion of composite structures in aircraft industry, the need of reliable repair techniques became a priority. Increasing efforts and research are now dedicated to this field. Composite patches on composite structures have their own failure modes and critical points. Unlike metallic structures, here there are not residual stresses between parent structure and patch, since the materials are the same. On the other hand, composite structures are more prone to other damages intrinsic of heterogeneous materials, such as resin microcracks around the removed damaged area that can propagate beneath the patch and reduce the overall resistance. The main problem related to patch repair though is the risk of debonding between the patch and the substrate, which usually begins from the tapered edges of the patch.

Two strategies have been experimented so far for this kind of SHM area. A first path, opened by White from Royal Melbourne Institute of Technology, suggested the use of piezoelectric devices to measure changes in the frequency response of the repaired structure due to the presence of debonding. In other words, it is a development of the tap test realized continuously in real time with the use of surface mounted transducers. This technique was first experimented on external doubler repairs [26], then it was extended to scarf repairs [27].

The second field of study involves the use of fiber Bragg grating sensors, whose effectiveness has been already proven with composite patches on metallic structures. Strain based health assessment of bonded composite repairs with FBGs was made by Li et al [28]. External doublers repair and scarf repair were examined. A finite element study showed that the strain in the region subject to debond changes significantly compared to the undamaged state. An experimental investigation was then conducted, trying to detect the presence of debond through the placement of 2 FBG sensors. As a result, debonds were detected by means of a differential strain approach, where difference of the strain felt by the two sensors increased with the debond length. However, the debond size could not be determined unless the structural loading was known, because the strain differential is a function of both the debond length and the applied load. This inconvenient could be solved by using a chirped FBG, that, being able to detect the strain decay to zero and its movement through the patch, could be able to determine the length of the debond. This was the main goal of present work.

3.2 Specimen Sizing

In order to understand the problems related to a structural repair, a preliminary study of a damaged and repaired specimen was made with the FEA software Abaqus. For this kind of work the shear and the stress out of plane play a very important role for the debond of the patch, including the interaction between one layer and another for the overall structure. For these reasons the solid elements model was preferred.

Before any evaluation, it is important to specify that everywhere in this dissertation the x axis is considered to be parallel to the load/displacement imposed, the y axis is perpendicular and planar to the specimen main surface and the z axis runs through the specimen thickness. Besides, every time a "length" is referred, it is something related to a boundary aligned with the x axis, while a "width" is related to the y axis; any dimension through the z axis is referred as a thickness.

The numerical analysis was performed on the specimens that would be used for the experimental tests. The fixed parameters for the specimen dimensioning were the following:

- The sensor length was fixed at 2 cm.

- The two clamps of the tensile testing machine had a width of 1 inch (about 2.54 cm), and a length of 2 inches (5.08 cm).
- The maximum length of the specimen, in order to fit into the tensile testing machine, was 45 cm.

The presence of a patch on a thin laminate generates a not negligible bending due to a load eccentricity that would increase the complexity of the problem and would not help for debond generation and growth. For this reason a sandwich material with a honeycomb that might increase the panel stiffness was chosen, with one of the two skin acting as the damaged laminate.

Sandwich materials require particular attention in case of a tensile test: without a proper solution, the two clamps of the tensile testing machine would crash by compression the core on the two edges. It is necessary then to insert inside the core some metal plugs, in order for the specimen to be safely fixed by the handles without causing any damage. This configuration is strictly necessary in case some information about the tensile behavior of the whole structure is required; however, it definitely increases the time required to produce each specimen. Since for this dissertation the focus was just on the interaction between patch and one skin, an alternative configuration was preferred: the parts subjected to clamping compression were reduced to only the repaired skin, eventually reinforced with fiber glass tabs. This way, it would possible to manufacture a single panel and all the specimens could be cut from the same panel without the need to prepare every specimen one by one. However, the main drawback of this method is the appearance of a bending due to load eccentricity. In order to minimize this effect it was necessary to reduce as much as possible the zone where core and second skin are removed.

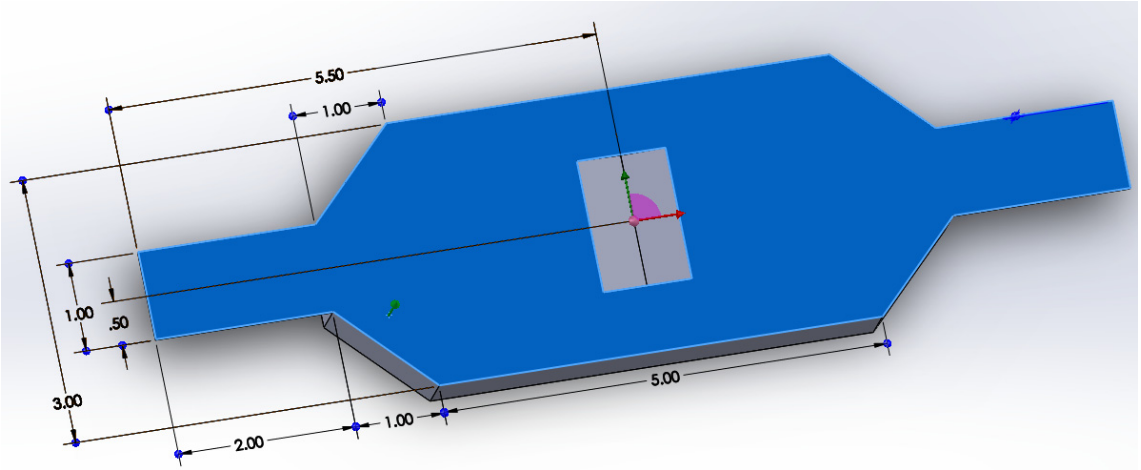

Figure 4: Damaged sandwich specimen.

Figure 4 represents the Solid Works part prepared to create the .DXF file used for the interface with the CNC machine. Clamping region was optimized to have a stress load as uniform as possible throughout the specimen. The whole specimen has the complete sandwich panel except for the 2x1 inches rectangles dedicated to the clamping. The specimen presents a central damage, created by an extruded cut with triangular shape.

3.3 Strain Field Analysis

In order to understand how to deal with the data output from the sensor, it was necessary to have a complete knowledge of the strain field all over the specimen and the patch, with special attention to the places where the sensor might be positioned. A parametric study was performed with different debond sizes, to see the effects on the strain field of an increase of the damage. The sensor should be positioned in a place where the

strain suffers the largest change due to this increase. This location was identified as the top surface of the patch. A node path was selected that ran over the whole patch length on the top surface, and the strain was captured for multiple debond sizes: no debond, 5 mm, 10 mm and 15 mm.

As expected, a sensible variation in strain was visible throughout the node path. Here, the strain starts at a low value, it rises until the part over the damage, it remains constant throughout the damage and then it starts decreasing until reaching approximately the same minimum value as the starting edge. The violet line corresponds to the completely bonded patch. The presence of a debond forces the strain to decrease to zero at the debond area: as debond size grows, the area with zero strain increases as well. Since the flat part in correspondence to the damage remains with the same size, the natural consequence is a steeper strain decrease. A secondary consequence is that as de-bonding grows, less strain is transferred from the damaged structure to the patch, and as a consequence the strain to which the damaged part is subjected will be higher, increasing the risk of damage growth. Then, a second parametric study was performed to evaluate the effect of a load change on the strain field.

The specimen analyzed numerically was produced using a wet lay up technique. A unique sandwich panel was built first, from which all the specimen were obtained with a CNC machine. The two clamping regions were strengthened with four fiber glass tabs, attached with structural adhesive. Damage was created with the CNC machine as well. One of the final damaged specimens is shown in figure 5.

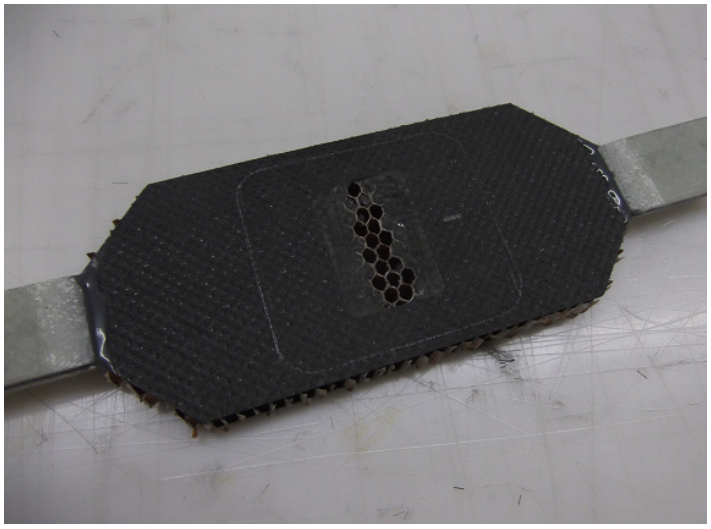

Figure 5: Sandwich specimen produced.

3.4 Experimental Results

Confirmed by the FEA analysis, the debond growth of the patch radically changes the strain field on the patch, because the debonded area has the strain that quickly decreases to zero. A sensor placed on top of a patch then, in case of debonding, should experience part of the grating not being stretched by any strain, with the rest still suffering the effect of the strain field. This situation was studied in depth to see the sensor response in this case. The sensors were preliminarily analyzed through the use of a heat source that could heat partially and gradually the sensor, in order to see its response when subjected to a variable partial change from the originary grating period.

In order to characterize the sensor behavior qualitatively and quantitatively, the following procedure was used. A heat gun was directioned perpendicularly at 20 cm distance at low power, and at every new test the aluminum plate was shifted uncovering 3 more millimeters of the sensor. Light was first injected to the fiber

without any heat, and the obtained spectrum was used as a reference for any further measurements. Heat was then applied and the light was sent through to measure the difference.

Two channels of data could be derived from the sensor, one relative to what happens at higher wavelengths (HW) and the other to what concerns the low wavelengths (LW) of the reflection spectrum; the excitation level of the two channels depends on the grade at which each area is affected by the induced change in the grating period. If the two areas are excited at the same level, such as when heat is applied to the whole sensor, the two channels respond the same way, leading to a rigid shift of the reflection spectrum rightwards. If instead the two channels are excited differently, such as for the case where only half of the sensor is heated, the differential between the high and low wavelength response will be unequal, leading to a reduction or an expansion of the reflection spectrum, respectively if the low wavelengths or the high wavelengths half is heated. The data, acquired as a shift in wavelength were calculated considering the difference in wavelength at which the spectrum crossed the line at -24dB with respect to the non-heated configuration, upwards for low wavelengths and downwards for high wavelengths. Gradual sensor attachment onto laminate.

The second step involved the use of a tensile testing machine to apply the strain to the sensor. A sensor was gradually attached to a laminate ready for being clamped on a tensile testing machine. This experiment had the objective of evaluating the sensor behavior when part of its physical length is subject to some strain and the rest is free. As expected, the linearized method presented higher errors, both at an absolute and at a relative level. Besides, when the debond size becomes relevant the error becomes negative, thus becoming non-conservative.

Patch Sensor on Top and Attached to Specimen

The following step was to set up a realistic configuration to test the actual functioning of the system. A specimen from the ones previously produced was taken, one skin was damaged and repaired with a composite patch. According to the FEA analysis, the configuration that showed a bigger change in the strain field when debonding occurs was the one with the sensor placed on the top of the patch, where the debonded part has the strain decreased to zero.

One of the most important goals of the tests was to see if the sensor is able to give an estimate of the debond size that may not require any information about the load to which the structure is subjected. In order to verify if this assumption is valid for the method here created, a specimen with a debond of around 4 mm was placed on the tensile testing machine, and it was subjected to ramp load from 0 to 5000 N. Every 1000 N the ramp was paused, light was injected through the fiber and the shifts of high and low wavelengths were measured.

If the sensor had exactly the property mentioned before, the black line representing the ratio between the green and the yellow line would be completely flat. Unfortunately, it presents a little constant slope, suggesting that this method can be used quite accurately but it must be calibrated with loads that may be as close as possible to the operating loads. With the sensor calibrated on a certain load value, and as calibrating it means establishing the value of a and b of the exponential method equation, if the load is higher than the one used for calibration then the estimate of the debond with be higher than the real one, and vice versa. For this reason, it would be very important to calibrate the sensor with the highest load that the structure is expected to bear, in order to have always a conservative estimate of the present debond. Nonetheless, if the calibration load is too far from the average load the average error will be higher. In this case, the exact value of HW/LW, obtainable using the real size of debond in the exponential equation, is 1.694, that can be met for a load between 4000 and 5000 N. For 5000 N the calculated debond is 3.47 mm, less than the real one, it is, a non-conservative error. On the contrary, for the previous tests, where the load was lower than 4000 N (3500 N), the estimate of debond had a positive error, 2.09 mm for a debond of 2 mm and 14.30 mm instead of 12 mm. For these reasons, it can be stated that the calibration achieved with heat tests is adapt for a structure that has to be subjected to a load that may never be much higher than 4500 N.

Fatigue Test

The final step tried was to create the debond as much realistically as possible, it is, through the application of a cyclic load to the damaged and repaired structure. It was important that, during the test, the patch debond from the skin might be the first damage to appear: in order for that to happen it was important that the specimen did not have any critical point, weakness or point of concentrated stress, to avoid any kind of nucleation of unwanted damage. Also, it was important that the debond would start around the area where the sensor was situated. For all these reasons a special patch design was required. In short, these two goals had to be pursued:

- Promote as much as possible the generation of a patch debond;
- Ensure that debond would start and grow from the sensor zone.

For this purpose it was possible to work on three variables: thickness, material and shape. As for the thickness, it is clear that an increase of thickness increases the peel stress on the patch edge where the sensor is located, although this effect is mitigated as the patch thickness assumes high values. Peel stress is also dependent on the patch stiffness: the Young module to be considered is the one of the direction of the imposed displacement, E_{xx}. Generally, a stiffer patch causes higher peeling stresses. Thus, a patch made of unidirectional plies was preferred. As for the shape, the two main features that can influence the stress field are the presence of sharp corners and the non-uniform width of the patch through the length: a reduction in width will generate a stress concentration on the shorter edge.

The patch was then attached to the specimen with epoxy resin, cured with the application of load through spring clamps. In order to promote the patch debond, a thin layer of pvc was added below the patch, preventing the first 2 mm of patch from being correctly attached. After the time required for the cure, the specimen was placed on a fatigue testing machine, and some cyclic load was applied.

3.5 Discussion

The overall objective of this work was to study and characterize the behavior of the CFBG sensor and analyse its applicability to the SHM of composite repairs. Details of the results will be discussed during the Lecture Series. More specifically, the capability of detecting the presence of a patch debond and evaluating its size was examined. FEA tests were performed to evaluate optimal configurations. These configurations were then processed, leading to two criteria to achieve the main goal: being able to estimate the size of the patch debond present with acceptable accuracy without any information about the load to which the structure is subjected. This criterion required a calibration, and provided good results. The second criterion does not need any calibration, and the error should be higher, although most of times conservative. Tests were performed at three levels, to evaluate the accuracy of these two criteria.

At a first level, a gradual sensor attachment to a laminate led to very good results, calculating the debond size with good accuracy. Errors were below 5% for the exponential method, a little higher for the linearized method.

At a second level, a sandwich specimen, damaged and repaired with a patch, was tested with a sensor on top of the patch. Debond was gradually produced manually/chemically, and for all the different stages light was injected and the two criteria were used to evaluate the size of debond. Again, although with some more noise, results were encouraging, especially for the exponential method. A parametric study with a same configuration and different loads highlighted that the calibration for this method should be done considering a load that might be as close as possible to the operational, higher than the operational level if a conservative error is wanted.

Finally, the fatigue test machine was used to try to produce the debond on another sandwich specimen. The patch was particularly designed to promote the nucleation of a debond near the sensored edge, and a strip of

pvc was inserted at one edge between the patch and the parent structure to facilitate the detachment. Unfortunately, no debond appeared for this last test. As a conclusion, it is possible to deduce from the work done that the objective of finding a method that may reach the goal fixed with the sensors available has been achieved.

Further study and tests would allow to gain more confidence on this method, applying it on other repairs and configurations, such as scarf repairs. The first step should include repeating the fatigue test with a specimen with a skin with increased thickness, at least doubled or tripled, so that the load can be higher and the strain cycles may be able to generate some patch detachment. The configuration with the patch embedded in the mid thickness of the patch could not be really analyzed in this work, although it is probably the most promising one in terms of possible future application in a real repair.

4.0 REFERENCES

[1] G. Zhou, Damage detection and assessment in fiber-reinforced composite structures with embedded fiber optic sensors-review, Smart Materials and Structures (2002).

[2] C. J. Keulen, M. Yildiz, A. Suleman, Multiplexed FBG and Etched Fiber Sensors for Process and Health Monitoring of 2-&3-D RTM Components, Journal of Reinforced Plastics and Composites 30 (2011) 1055-1064.

[3] K. Kuang, Use of conventional optical fibers and fiber Bragg gratings for damage detection in advanced composite structures: a review, Applied Mechanics Reviews (2003).

[4] C. Doyle, A. Martin, T. Liu, M. Wu, In-situ process and condition monitoring of advanced fiber-reinforced composite materials using optical fiber sensors, Smart Materials and Structures (1998).

[5] N. Takeda, Characterization of microscopic damage in composite laminates and real-time monitoring by embedded optical fiber sensors, International Journal of Fatigue (2002).

[6] S. Yashiro, N. Takeda, T. Okabe, H. Sekine, A new approach to predicting multiple damage states in composite laminates with embedded FBG sensors, Composites Science and Technology 65 (2005) 659-667.

[7] N. Takeda, S. Yashiro, Estimation of the damage patterns in notched laminates with embedded FBG sensors, Composites Science and Technology (2006).

[8] Z. Su, L. Ye, Y. Lu, Guided Lamb waves for identification of damage in composite structures: A review, Journal of Sound and Vibration 295 (2006) 753-780.

[9] A. Othonos, K. Kalli, G. E. Kohnke, Fiber Bragg Gratings: Fundamentals and Applications in Telecommunications and Sensing, Artech House Inc., Boston, Massachusetts, (1999).

[10] B. Harris, Fatigue in composites, Woodhead Publishing Limited, Cambridge, England, (2003).

[11] S. W. Tsai, S. Ha, T. E. Tay, Y. Miyano, S. Shin, Strength & Life of Composites, Aero & Astro, Stanford U, (2008).

[12] J. Degrieck, W. Van Paepegem, Fatigue damage modeling of fiber reinforced composite materials: Review, Applied Mechanics Reviews 54 (2001) 279.

[13] V. Natarajan, H. Gangarao, Fatigue response of fabric-reinforced polymeric composites, Journal of Composite Materials (2005).

[14] C. Shin, Fatigue damage monitoring in polymeric composites using multiple fiber Bragg gratings, International Journal of Fatigue (2006).

[15] A. Rotem, A Fatigue Failure Criterion for Fiber Reinforced Materials, Journal of Composite Materials (1973).

[16] H. Whitworth, A stiffness degradation model for composite laminates under fatigue loading, Composite structures (1997).

[17] H. A. Whitworth, Modeling Stiffness Reduction of Graphite/Epoxy Composite Laminates, Journal of Composite Materials 21 (1987) 362-372.

[18] J. Yang, D. Jones, S. Yang, A stiffness degradation model for graphite/epoxy laminates, Journal of Composite Materials (1990).

[19] W. Hwang, Fatigue of composites: fatigue modulus concept and life prediction, Journal of Composite Materials (1986).

[20] W. Hwang, K. Han, Cumulative Damage Models and Multi-Stress Fatigue Life Prediction, Journal of Composite Materials 20 (1986) 125-153.

[21] L. Lee, K. Fu, J. Yang, Prediction of fatigue damage and life for composite laminates under service loading spectra, Composites Science and Technology 56 (1996) 635-648.

[22] H. A. Whitworth, Cumulative Damage in Composites, Journal of Engineering Materials and Technology 112 (1990) 358.

[23] N. Takeda, S. Yashiro, T. Okabe, Estimation of the damage patterns in notched laminates with embedded FBG sensors, Composites Science and Technology 66 (2006) 684-693.

[24] Y. Okabe, T. Mizutani, S. Yashiro, N. Takeda, Detection of microscopic damages in composite laminates with embedded small-diameter fiber Bragg grating sensors, Composites Science and Technology (2002).

[25] S. Yashiro, T. Okabe, Estimation of fatigue damage in holed composite laminates using an embedded FBG sensor, Composites Part A: Applied Science and Manufacturing (2011).

[26] White Caleb, Whittingham Brendan, Li Henry C. H, Herszberg Israel, and Mouritz Adrian P. Health assessment of bonded composite repairs with frequency response techniques. Proc. SPIE, 6414:64140W–64140W–8, 2006.

[27] C. White B. Whittingham H. Li C.H. Herszberg M.A. Israel. Vibration based structural health monitoring of adhesively bonded composite scarf repairs. 5th Australasian Congress on Applied Mechanics (ACAM 2007), 10-12 December 2007.

[28] Henry C.H. Li, Felix Beck, Olivier Dupouy, Israel Herszberg, Paul R. Stoddart, Claire E. Davis, and Adrian P. Mouritz. Strain-based health assessment of bonded composite repairs. Composite Structures, 76(3):234 – 242, 2006. US Air Force Workshop Health Assessment of Composite Structures. Health Assessment of Composite Structures.